Fachtagung "Experimentelle Strömungsmechanik"
5. – 7. September 2017, Karlsruhe

Attraktoren für die Bewegung von Teilchen mit endliche Größe in einem angetriebenen Rechteckbehälter

Attractors for the motion of finite-size particles in a lid-driven cavity

Haotian Wu[1], Francesco Romanò[1], and Hendrik C. Kuhlmann[1]
[1]Institute of Fluid Mechanics and Heat Transfer, TU Wien, Getreidemarkt 9, Tower BA/E322, 1060 Vienna, Austria

Behälterströmung, KAM-Tori, Einzelpartikelverfolgung
Cavity flow, KAM tori, single-particle tracking

Abstract

The motion of a spherical particle in a two-sided lid-driven cavity is investigated experimentally and numerically for moderate Reynolds numbers, for which the flow is steady and three-dimensional. Periodic attractors for the motion of a suspended particle have been found for certain combinations of Reynolds number and particle size.

Introduction

In the present study we illustrate a mechanism of attraction for finite-size particles in a two-sided lid-driven cavity flow mainly induced by particle-boundary interaction. On an increase of Reynolds number, the flow in a rectangular cavity driven by two facing walls moving tangentially in opposite direction bifurcates from a steady two-dimensional flow to a three dimensional spatially periodic convective cellular flow (Kuhlmann et al. 1997), where the flow is subdivided in regions of chaotic and regular streamlines. The regular region appears in form of Kolmogorov-Arnold-Moser (KAM) tori (Ottino 1989). When a finite-size and neutrally-buoyant particle is transported near a moving boundary, strong repulsion forces due to the particle-boundary interaction can transfer the particle from the chaotic to the regular region (Romanò & Kuhlmann 2016). For suitable Reynolds numbers and particle sizes, this dissipative effect can cause a rapid attraction of the particle to a periodic attractor, which is located inside a regular region of the flow (Kuhlmann et al. 2016).

Three-dimensional particle tracking is used to reconstruct the trajectory of a single particle. The existence of different attractors and their properties are established experimentally. A theoretical explanation and a numerical confirmation of the phenomenon is provided on the basis of the streamline topology and the particle-surface interaction model (Romanò & Kuhlmann 2016, Mukin & Kuhlmann 2013, Hofmann et al. 2011).

Experiment Setup

The flow in the cavity is driven by the moving surfaces of two cylinders with radius R = 135mm, which can rotate independently about their axes with angular velocity Ω, as shown in Fig. 1. The height of the cavity is H = 40mm, while span-wise length L is 435mm. The minimum and maximum widths of the cavity are, respectively, W_{min} = 63mm and W_{max} = 65mm,

Karlsruhe, Germany, ISBN 978-3-9816764-3-3

which leads to a mean aspect ratio $\Gamma = 1.6$. Silicone oil with kinematic viscosity v = 20cSt and density ρ_f = 0.95g/cm^3 at T = 25°C is used as the working fluid. The particles employed are high-density polyethylene spheres, which are nearly density-matched to the fluid. The particle has a radius a of 2mm and density of 0.94g/cm^3.

Two synchronized cameras are used to capture the particle motion from the side and top view of the cavity using a frame rate of 20Hz. With image processing, the three-dimensional trajectory of the particle centroid can be reconstructed. The processing involves four steps to determine the particle centroid (see Fig. 2): (a) the original image is converted to a gray-scale image using a blue-yellow colormap, where the particle is identified as a bright yellow region, (b) from each frame a background image obtained by averaging 200 frames is subtracted, (c) noise in each image is reduced by applying a convolution with a Gaussian low pass filter, (d) by setting a color threshold the resulting image is convert to a binary field, where the pixel values in the region occupied by the particle are allocated to ones, while the background pixels are set to zero. The particle centroid is then determined by calculating the centroid of binary field.

The error of this particle tracking technique can be estimated by comparing the x coordinates of the particle centroid measured from the side and from the top view of the cavity, as shown in Fig. 3. The maximum relative difference between the x coordinate measured from both views is less than 2%, which can be regarded as the measurement error.

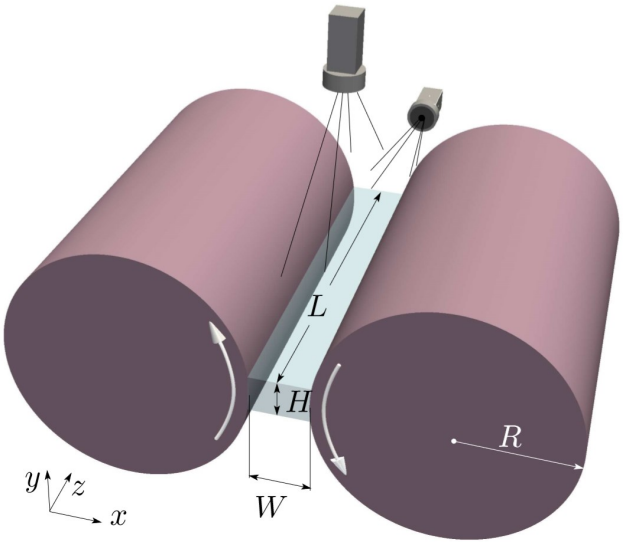

Fig. 1: Sketch of experiment setup and coordinate system of the cavity. Arrows indicate the direction of rotation of the cylinders.

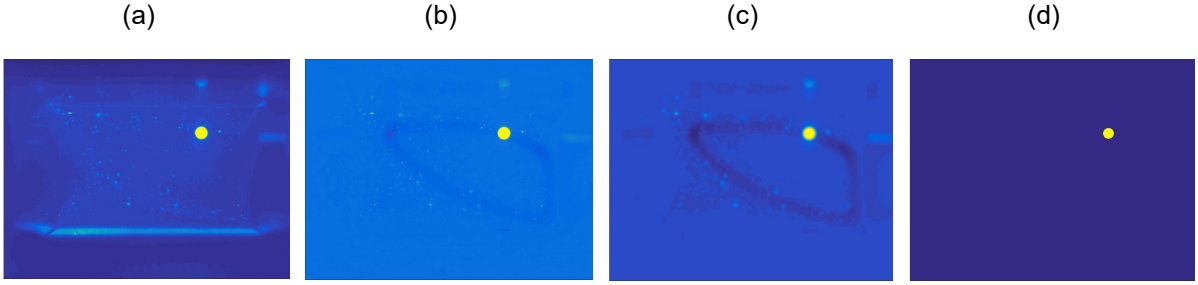

Fig. 2: Image processing of single particle tracking: (a) original image, (b) subtraction of a background image, (c) Gaussian low-pass filtering, (d) binary image obtained by setting a color threshold.

Karlsruhe, Germany, ISBN 978-3-9816764-3-3

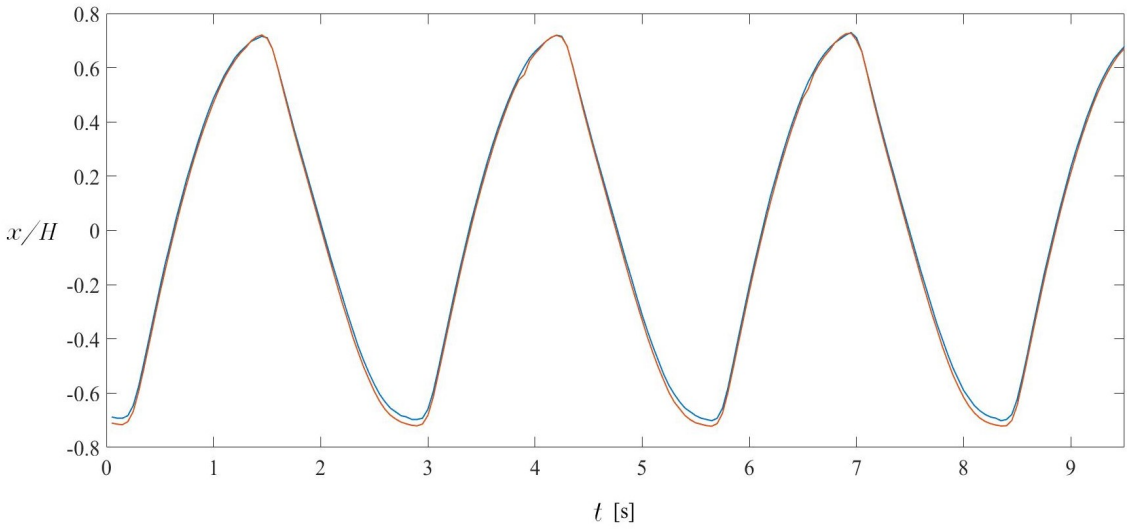

Fig. 3: The *x* components of the particle centroid measured from side view (red) and from top view (blue) of the cavity as functions of time.

Results and discussion

The steady three-dimensional convective cellular flow in the two-sided lid-driven cavity is mirror symmetric with respect to the cell boundaries, while in each individual convective cell, the flow is point symmetric with respect to the cell centre. Numerical simulations (Romano et al. 2017) reveal the co-existence of regular and chaotic flow regions. A single pair of point symmetric KAM tori was found in each individual convective cell at Re = 400, as shown in Fig. 4.

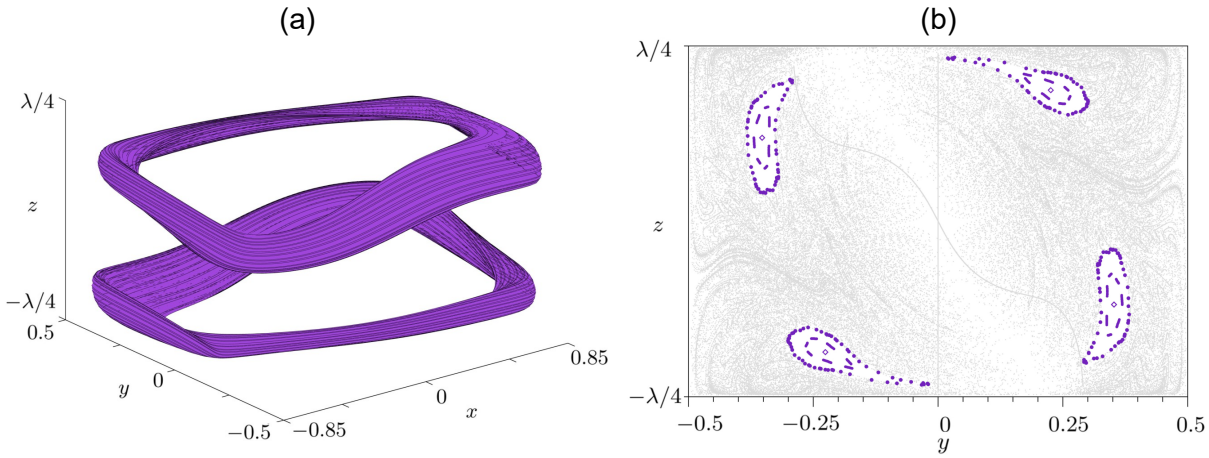

Fig. 4: Flow topology for two-sided lid-driven cavity flow at Re = 400 (Romano et al. 2017): (a) Largest reconstructible KAM-tori in one individual convective cell, (b) Poincaré section of 2500 streamlines on the plane *x* = 0.5. Purple islands indicate stream tubes on KAM tori, while gray dots represent the chaotic region.

It has been observed that when a finite-size particle is transported near the moving wall, it experiences a repulsive force, which rapidly decelerates the particle to a zero wall normal velocity. After this nearly impulsive interaction the particle slides almost parallel to the wall within a nearly constant distance Δ until it is released back to the bulk, see Fig. 5. The distance Δ comprises of the particle radius *a* plus the lubrication-gap width δ between particle's surface and the moving wall.

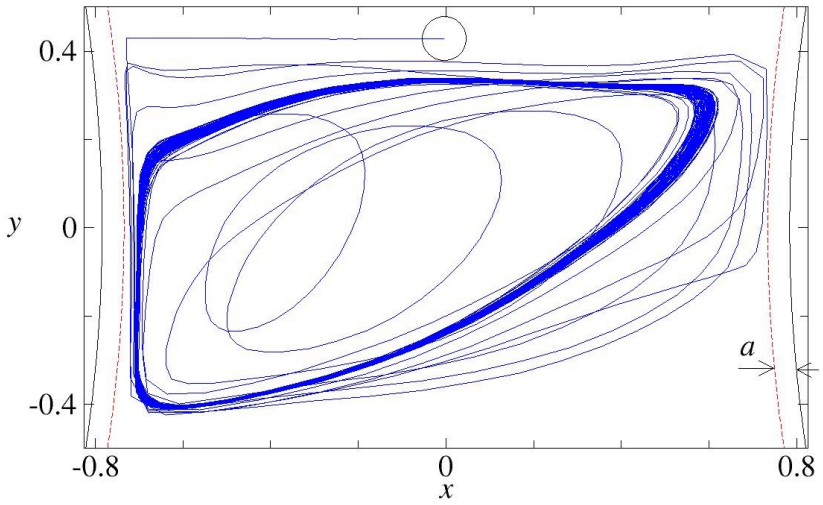

Fig. 5: Projection of a single particle trajectory onto the (x,y)-plane. Initially the particle is advected in the chaotic region of the flow. After several revolutions and interaction with the walls, it is attracted to a limit cycle (densely populated closed orbit). Here a = 2mm, Re = 400. The motion is counter-clockwise. The circle indicates the particle size at its initial position.

Here we consider a particle radius a = 2mm and Re = 400. After several particle-boundary interactions we find the particle to settle on one of the two point symmetric limit circles shown in Fig. 6. In the case shown the limit cycle practically coincides with the closed streamline inside each of the point symmetric KAM tori. In such particular case, the closed streamline of the KAM-tori approaches the moving wall up to a minimum distance $\Delta = a + \delta$. Once the particle is released to the regular region, it is focussed to the closed streamline by the process described in Hofmann & Kuhlmann (2011).

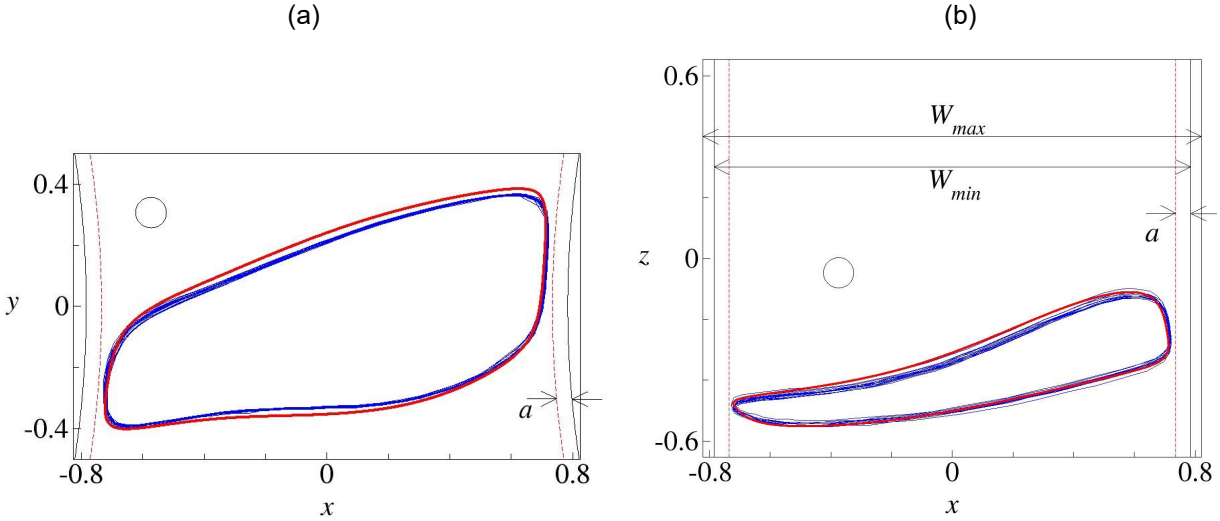

Fig. 6: Single-particle (a = 2.00mm) trajectory (blue, measurement) in a nearly rectangular cavity making 15 revolutions about one limit cycle during t ∈ [65,105]s after Re was relaxed to 400, and closed streamline (red, numerical simulation). The circle indicates the particle size. Results are scaled using the height of cavity H. Shown are projections onto the (x,y)-plane (a) and the (x,z)-plane (b).

The reproducibility of the limit cycle is proven by repeating 62 experiments with a single particle. In order to realize random initial positions for the particle, the Reynolds number is increased to Re = 1600 to drive the flow into a fully chaotic state. After 60s Re is decreased sharply to Re = 400. The particle is finally attracted to one of the limit circles in different con-

vective cells, like those shown in Fig. 7a. Since the flow is periodic and mirror symmetric with respect to the cell boundaries, all closed streamlines and particle limit cycles in different convective cells can be mapped to the two generic limit cycles of a single cell. A superposition of 62 single-particle trajectories (blue) mapped to the generic convective cell are shown in Fig. 7b in comparison with the closed streamlines (red). The latter were obtained by numerical simulation. The shape and the location of the particle limit cycles compare very well with the closed streamlines. However, the two sets of limit cycles are not exactly point symmetric with respect to the cell centre as are the closed streamlines. This effect might be due to buoyancy forces caused by the small density mismatch of the order of 1% between the particle and the working fluid.

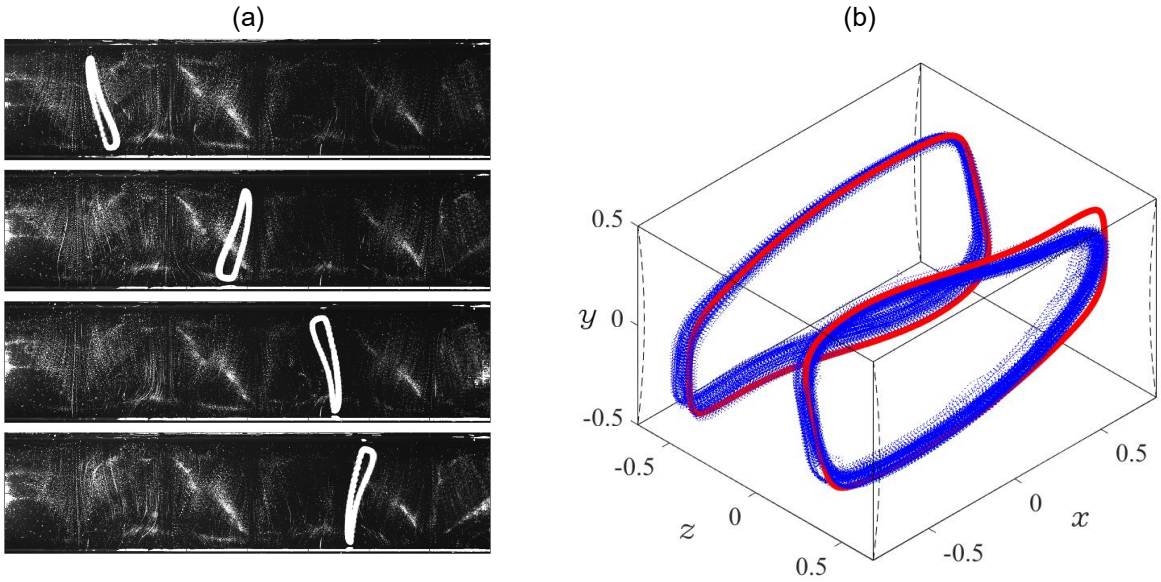

Fig. 7: (a) Long-time-exposure images from the top view of the cavity showing particle trapping in different convective cells. The cells can be identified by fine streaklines made by small aluminium flakes. (b) 62 particle trajectories (blue, measurements) and closed streamlines (red, numerical simulation) inside the KAM tori (not shown).

Conclusion

Attractors induced by particle-boundary interaction have been found in a two-sided lid-driven cavity for finite-size particles. The shape and location of the particle attractors are in good agreement with the closed streamlines of the KAM tori obtained by numerical simulation. Since the density of the particle cannot perfectly be match with working fluid, particles with various density ratio need to be investigated in order to clarify the effects of buoyancy and/or inertia on the particle motion.

References

Hofmann, E., Kuhlmann, H.C., 2011: Particle accumulation on periodic orbits by repeated free surface collisions. Phys. Fluids, 23: 072106

Kuhlmann, H.C., Wanschura, M., and Rath, H.J., 1997: Flow in two-sided lid-driven cavities: non-uniqueness, instabilities, and cellular structures. J. Fluid Mech., 336: 267–299

Kuhlmann, H.C., Romanò, F., Wu, H., Albensoeder, S., 2016: Particle-motion attractors due to particle-boundary interaction in incompressible steady three-dimensional cavity flow. In 20th Australasian Fluid Mechanics Conference, Book of Abstracts p. 102, paper no. 449 (4 pages)

Mukin, R.V., Kuhlmann, H.C., 2013: Topology of hydrothermal waves in liquid bridges and dissipative structures of transported particles. Phys. Rev. E, 88: 053016

Ottino, J.M., 1989: The Kinematics of Mixing: Stretching, Chaos, and Transport. Cambridge Texts in Applied Mathematics. Cambridge University Press, Cambridge
Romanò, F., Kuhlmann, H.C., 2016: Numerical investigation of the interaction of a finite-size particle with a tangentially moving boundary. Int. J. Heat Fluid Flow, 62: 75–82
Romanò, F., Kuhlmann, H.C., Albensoeder, S., 2017: Topology of three-dimensional steady cellular flow in a two-sided anti-parallel lid-driven cavity. J. Fluid Mech., accepted